In vitro ageing of myotubes derived from myoblasts of patients affected by myotonic dystrophy type 2: ultrastructural evidence

M. Giagnacovo,[1] M. Costanzo,[1] R. Cardani,[2,3] P. Veneroni,[1] C. Pellicciari,[1] G. Meola[4]

[1]Dipartimento di Biologia Animale, Laboratorio di Biologia cellulare e Neurobiologia, Università di Pavia, Italy; [2]Dipartimento di Biologia molecolare e Biotecnologie, [3]Centro per lo studio delle Malattie Neuromuscolari-CMN, and [4]Dipartimento di Neurologia, IRCCS Policlinico San Donato, Università degli Studi di Milano, Italy

Corresponding author: Marzia Giagnacovo
Dipartimento di Biologia Animale, Università degli Studi di Pavia, Via A. Ferrata 9, 27100 Pavia, Italy
Tel. +39.0382.986417 - Fax +39.0382.986325.
E-mail: marzia.giagnacovo@unipv.it

Summary

Myotonic dystrophy type 2 (DM2) is a dominantly inherited autosomal disease with multi-systemic clinical features and is caused by expansion of a CCTG tetranucleotide repeat in the first intron of the zinc finger protein 9 (ZNF9) gene in 3q21. The expanded-CCUG-containing transcripts are retained in cell nuclear domains (called foci) which specifically sequester some splicing factors, thus causing a general alteration of the pre-mRNA post-transcriptional pathway that is likely responsible for the multifactorial phenotype of DM2 patients. However, at the skeletal muscle level, there is still no mechanistic explanation for the muscle weakness and atrophy of DM2 patients. It has been noted that in DM2 patients skeletal muscle regeneration is decreased, suggesting an impaired responsiveness of satellite cells to regeneration stimuli as much as it occurs in ageing muscles. In order to investigate the differentiation potential of senesceing DM2 myoblasts and the development of the derived myotubes, we developed a model system of cell ageing *in vitro*: by this approach, the structural features of myotubes derived from DM2 myoblasts grown in culture for increasing times have been investigated by fluorescence and transmission electron microscopy. Apparent alterations of several cytoplasmic features have been observed in the myotubes derived from myoblasts at higher passages. This strongly argues in favour of the involvement of satellite cell senescence in the reduced regenerative potential of dystrophic muscles.

Key words: myotonic dystrophy type 2-DM2, myoblast, myotube, cell senescence, fluorescence microscopy, electron microscopy.

Introduction

Myotonic dystrophy type 2 (DM2) is a dominantly inherited autosomal disease with multi-systemic clinical features and is caused by the expansion of a CCTG tetranucleotide repeat in the first intron of the zinc finger protein 9 (ZNF9) gene in 3q21 (Liquori *et al.*, 2001). The expanded-CCUG-containing transcripts are retained in the cell nucleus and accumulate in the form of focal aggregates (Liquori *et al.*, 2001): these nuclear foci of mutant mRNA specifically sequester essential splicing factors such as muscleblind-like (MBNL) proteins (Fardaei *et al.*, 2002, Cardani *et al.*, 2006, Pascual *et al.*, 2006), snRNPs and hnRNPs (Perdoni *et al.*, 2009a,b), leading to nuclear depletion and loss of function of these regulators (Mankodi *et al.*, 2001). This strongly supports the hypothesis that a general alteration of the pre-mRNA post-transcriptional pathway could be at the basis of the multifactorial phenotype of DM2 patients (Wheeler and Thornton, 2004; Ranum and Cooper, 2006).

However, at the skeletal muscle level, there is still no mechanistic explanation for the muscle weakness and atrophy of DM2 patients, or for the histopathological features of this disease which include fibre atrophy-hypertrophy, increased number of centrally located nuclei, and presence of fibres with nuclear clumps. It has been noted that in DM2 patients skeletal muscle regeneration is decreased in response to the ongoing muscle loss and dystrophy (Harper *et al.*, 2001); it is possible

that this poor repair response may result from impaired myogenesis in the adult DM2 muscle. Interestingly, DM muscle shares apparent similarities with the ageing muscle where the progressive muscle weakness and atrophy is accompanied by a slower regenerative capability (Schultz and Lipton, 1982; Machida and Narusawa, 2006; Verdijk et al., 2007).

In skeletal muscles, the myoblasts precursor cells called satellite cells provide the potential for both pre- and post-natal growth, as well as for muscle regeneration following injury (Moss and Leblond, 1971). It has been conclusively demonstrated that myoblast precursor cells, which are quiescent in normal muscles, become activated following injury: they then proliferate and fuse into myotubes which finally differentiate and become muscle fibres (Bischoff and Heintz, 1994; Cooper et al., 1999). It is likely that a failure in satellite cell activation or a change in the behaviour of the activated satellite cells could contribute to the development of the dystrophic phenotype of DM2 skeletal muscles.

In vitro myoblast cultures derived from human satellite cells provide a suitable and unique model for studying DM2 muscular precursor cells, and can be used to elucidate the molecular and cellular mechanisms involved in the pathogenesis of this disease (Mankodi et al., 2003; Cardani et al., 2004).

The aim of this study was to investigate, by fluorescence and transmission electron microscopy, the structural features of differentiating myotubes derived from DM2 myoblasts grown in culture for increasing lengths of time, in order to investigate the differentiation potential of senesceing myoblasts and the development of the derived myotubes.

Materials and Methods

Sample collection and cell culture

The biopsies used in this study were taken, under sterile conditions, from the biceps brachii of two DM2 patients, after informed consent. The histological diagnosis was performed on serial sections processed for routine histological or histochemical staining, based on the clinical criteria set by the International Consortium for Myotonic Dystrophies (Moxley et al., 2002). The biopsies from donors were trimmed of blood vessels, fat and connective tissues, and rinsed in phosphate-buffered saline (PBS); satellite cells were isolated as reported in Cardani et al. (2009) and placed in HAM's F10 medium (Sigma-Aldrich, Buchs, Switzerland) supplemented with 15% fetal bovine serum (Gibco, Invitrogen, Milan, Italy), 0.5 mg/mL bovine serum albumin (BSA), 0.5 mg/mL fetuin, 0.39 μg/mL dexamethasone, 10 ng/mL epidermal growth factor, 0.05 mg/mL insulin, 3 mg/mL glucose, 100 U/mL penicillin and 100 μg/mL streptomycin (all these reagents were from Sigma-Aldrich). The myoblasts obtained by this procedure were propagated in plastic flasks at 37°C in a humidified 95% air / 5% CO_2 atmosphere.

Proliferating myoblasts at the 9th (M9) and 12th passage (M12) in culture were used (their S-phase index being about 10% and 3%, as preliminarily estimated by BrdU incorporation experiments, not shown). M9 and M12 myoblasts were plated onto glass coverslips, and allowed to grow until they were 80% confluent. To initiate differentiation, the proliferative medium was replaced with differentiation medium consisting of DMEM supplemented with 7% FBS, containing 100 U/mL penicillin and 100 μg/mL streptomycin. Myoblasts were allowed to fuse and differentiate into myotubes for 8 (T8), 12 (T12), and 22 (T22) days.

Light microscopy

For fluorescence cytochemistry, myotube cultures were fixed with 4% formaldehyde in PBS for 15 min at 4°C, washed in PBS at room temperature, and incubated with either an Alexa 488-conjugated phalloidin (Molecular Probes, Invitrogen, Milan, Italy) diluted 1:40, or a mouse monoclonal antibody recognizing fast-myosin (Sigma-Aldrich), diluted 1:400, finally revealed with an Alexa 594-conjugated secondary anti-mouse IgG (Molecular Probes). All these reagents were diluted in PBS containing 0.1% BSA and 0.05% Tween-20 for 60 minutes at room temperature. After washing in PBS, cells were counterstained for DNA with Hoechst 33258 (Sigma-Aldrich; 1 μg/mL for 5 min), and mounted in a drop of Mowiol (Calbiochem, Milan, Italy).

For fluorescence microscopy, an Olympus BX51 microscope equipped with a 100W mercury lamp was used, under the following conditions: 330-385 nm excitation (excf) filter, 400 nm dichroic mirror (dm), and 420 nm long-pass filter, for Hoechst 33258; 450-480 nm excf filter, 500 nm dm, and 515-550 nm band-pass filter for Alexa 488; 550 nm excf filter, 590 nm dm, and 620 nm long-pass filter for Alexa 594. Images were recorded with a Camedia 5050 digital

camera system, and stored on a PC by the Olympus software, for processing and printing.

A cytochemical assessment of mitochondrial activity was also performed by vital staining with 2 μM JC-1 (5,5V,6,6V-tetrachloro-1,1V,3,3V-tetraethyl-benzimidazolcarbocyanine iodide; Molecular Probes, Invitrogen, Italy) for 15 min at 37°C in a 5% CO_2 atmosphere. When administered to living cells, JC-1 accumulates in the mitochondria where it emits either red or green fluorescence, depending on the mitochondrial membrane potential, the red signal indicating polarized mitochondria, and the green signal the depolarized ones (Reers *et al.*, 1991); therefore, the shift from red to green fluorescence is considered a reliable indication of a drop in the mitochondrial membrane potential. JC-1 positivity was visualized under the fluorescence microscope using a 450-480 nm excf filter, 500 nm dm, and 520 nm long-pass filter.

Transmission electron microscopy

T8, T12 and T22 myotubes were fixed with 2.5% glutaraldehyde and 2% paraformaldehyde in 0.1 M Sörensen phosphate buffer at 4°C for 1 h, washed, post-fixed with 1% OsO_4 at room temperature for 1 h, dehydrated with acetone and embedded in Epon: gelatine capsules were filled with the resin and placed up-side down onto the coverslips; after polymerization, the glass coverslips were detached by immersion in liquid nitrogen. Ultrathin sections were stained with uranyl acetate and lead citrate, and finally observed in a Philips Morgagni TEM operating at 80kV and equipped with a Megaview II camera for digital image acquisition.

Results

Transmission electron micrographs of myotubes derived from M9 myoblasts at the differentiation steps T8, T12 and T22 are shown in Figure 1. In the thin sections, T8 myotubes from M9 myoblasts showed elongated shapes, with longitudinally arranged nuclei (Figure 1a) (about 25% of the myotubes in the cultures showed more than 5 nuclei); in the cytoplasm, several bundles of longitudinally arranged myofibrils mainly occurred at the cell periphery, and frequently showed sarcomere-like figures (Figure 1c), consistent with the evidence after immunolabeling for fast-myosin (Figure 2a). Numerous elongated mitochondria with lamellar

cristae and some osmiophilic granules in their matrix were either orderly arranged between myofibril bundles or clustered around the nuclei (Figure 1b). Large amounts of ribosomes were present, mostly free in the cytoplasm but also in association with the cisternae of the endoplasmic reticulum. Well developed Golgi complexes often occurred close to the cell nuclei. A well developed smooth endoplasmic reticulum was ubiquitously distributed, mostly in the form of small round vesicles. Many lysosomes and residual bodies with different size and content were also observed. The cell nuclei were generally elongated, with low amounts of condensed chromatin and a single reticular nucleolus (Figure 1a).

Some ultrastructural features of T12 myotubes from M9 myoblasts were different from those observed in the thin sections of T8 myotubes. In detail: the myofibril bundles appeared less numerous and thinner, although they still showed sarcomere-like arrangements (Figure 1d); the mitochondria exhibited well developed cristae and many osmiophilic granules (Figure 1d); the residual bodies markedly increased in number, and roundish cytoplasmic areas appeared to be filled with a finely granular electron-dense material (Figure 1e). Similarly to T8, cell nuclei were lined along the longitudinal axis of the myotubes (not shown).

In T22 myotubes from M9 myoblasts, thin myofibril bundles were present, which still showed some sarcomere-like arrangements but were more irregularly arranged (Figure 1f,g and Figure 2b): instead of running parallel, they could be convergent and sometimes even perpendicularly oriented (Figure 2c). Mitochondria were smaller and contained a few cristae (Figure 1g). The smooth endoplasmic reticulum and the heterogeneous residual bodies became prominent, and large cytoplasmic areas were filled with electron-dense fine granular material. Finally, in the majority of thin sections, only one nucleus was observed in the cytoplasm, with the same ultrastructural features as in T8 and T12 myotubes (not shown). This likely relates with the increasing length of the myotubes, since the mean number of nuclei per myotube did not change significantly from T8 to T22 (3.5 and 3.9 nuclei per myotube, respectively).

Figure 3 shows myotubes derived from M12 myoblasts at the differentiation steps T8, T12 and T22. In the thin sections, T8 myotubes from M12 myoblasts were ovoid in shape, with one to three roun-
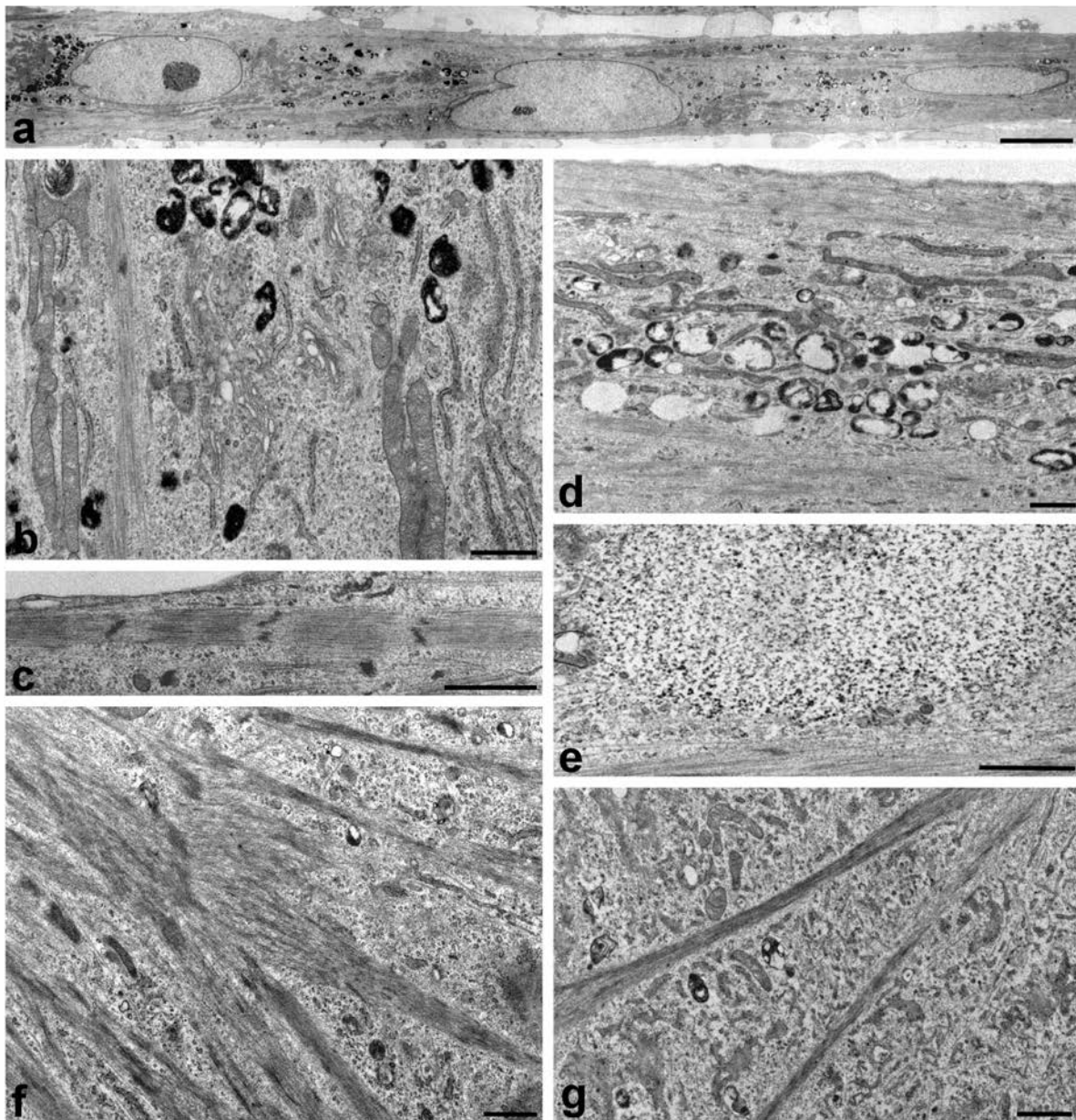
Figure 1. Electron micrographs of myotubes derived by M9 myoblasts at the differentiation step T8 (a-c), T12 (d,e) and T22 (f,g). (a) Myotube with three aligned nuclei. (b) Large amounts of free ribosomes, RER, well developed Golgi complexes, elongated mitochondria with lamellar cristae, and residual bodies occur in the myotube cytoplasm. (c) Detail of bundles of longitudinally arranged myofibrils showing sarcomerik-like arrangements. (d) In T12 myotubes the myofibril bundles still show sarcomeric-like arrangements, mitochondria contain many osmiophilic granules and residual bodies are prominent. (e) Cytoplasmic area filled with fine electron-dense granular material. (f,g) In T22 myotube the myofibril bundles are irregularly arranged and mitochondria are small with a few cristae; free ribosomes, rough and smooth endoplasmic reticulum are abundant. Bars: (a) 5 μm, (b-g) 1 μm.

dish or irregularly shaped nuclei often lined transversally to the longitudinal axis of the cell (Figure 3a). In their cytoplasm, areas containing the usual organelles were found close to wide, electron-lucent regions containing heterogeneous vacuoles (Figure 3b). Myofibril bundles were scarce in number and very thin, and sarcomere-like arrangements were rarely observed (Figure 3c); moreover, they seldom had a regularly longitudinal orientation. Small elongated mitochondria with a few cristae were mostly distributed as clusters (Figure 3c). Large amounts of free ribosomes, many rough endoplasmic reticulum cisternae, and well developed Golgi complexes were present. Smooth endoplasmic reticulum, lysosomes and heterogeneous vacuoles were abundantly and ubiquitously distributed. The cell nuclei generally contained scarce condensed chromatin and one reticular nucleolus.

T12 and T22 myotubes from M12 myoblasts were characterised by more numerous large electron-lucent cytoplasmic areas containing heterogeneous vacuoles, and by the scarcity of myofibrils arranged in bundles (Figure 3e). Some mitochondria showed the usual morphology, whereas other appeared to be swollen and contained hardly recognizable cristae (Figure 3d). After JC-1 staining, most of the mitochondria predominantly emitted red fluorescence (not shown), thus indicating that they were still functioning and preserved their intermembrane potential. Free ribosomes, rough endoplasmic reticulum and Golgi complexes were restricted only to limited cytoplasmic areas (Figure 3d), whereas the smooth endoplasmic reticulum and the heterogeneous vacuoles were prominent throughout the cytoplasm. The cell nuclei generally showed scarce condensed chromatin and one reticular nucleolus.

Conclusions

Taken together, our observations demonstrate that the myotubes derived from DM2 myoblasts at the earlier culture passage (M9) underwent differentiation and showed the structural features already described for myotubes from normal myoblasts (Curci *et al.*, 2008; Bigot *et al.*, 2008). During their ageing in culture, these myotubes exhibited a progressive disorganization of the cytoskeletal apparatus and, to a lesser extent, a decrease in mitochondrial functions, as suggested by the loss
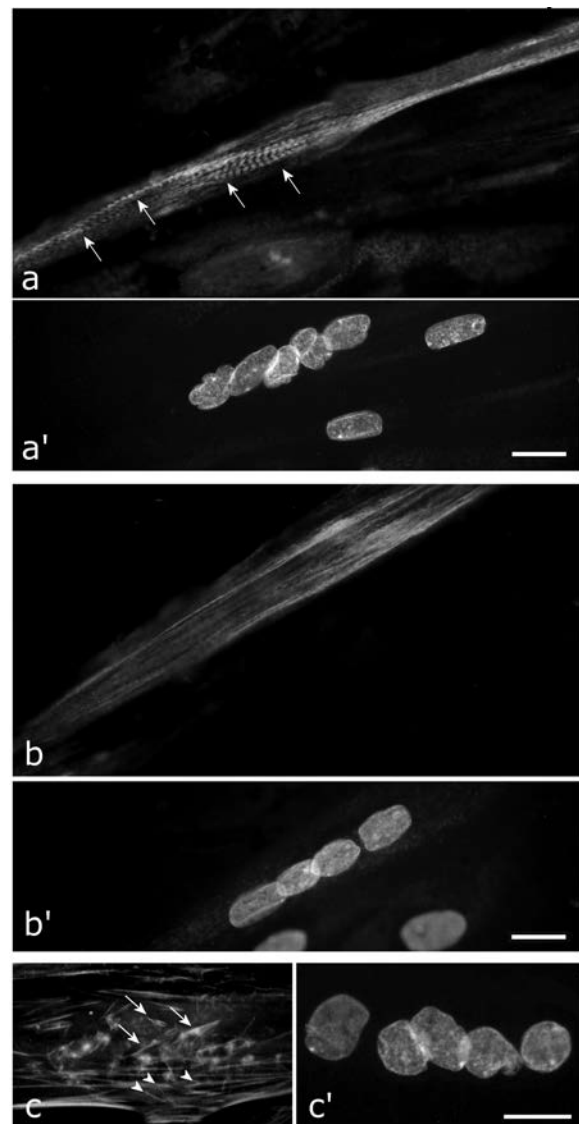
Figure 2. (a) A T8 myotube from M9 myoblasts is shown, after immunolabeling for fast-myosin: the arrows point to bundles of longitudinally arranged myofibrils; nuclear DNA was stained with Hoechst 33258 **(a')**. **(b)** A T22 myotube from M9 myoblasts after immunolabeling for fast-myosin and counterstaining of DNA with Hoechst 33258 **(b')**: myofibril organization is no longer visible. **(c)** Detail of a T22 myotube from M9 myoblasts after labeling of F-actin with phalloidin: actin bundles are irregularly arranged (arrows), and sometimes become convergent and perpendicularly oriented (arrowheads); nuclear DNA was stained with Hoechst 33258 **(c')**. Bars: 20 µm

of cristae and the concomitant accumulation of osmiophilic granules in their matrix (Jacob *et al.*, 1994; Malatesta *et al.*, 2001). Conversely, the proteosynthetic apparatus did not show massive morpho-functional alterations. Smooth vesicles and heterogeneous vacuoles markedly increased as it was observed to occur during cell senescence, in parallel with progressive malfunctioning of the degradation systems (Jameson, 2004).

As reported by Bigot *et al.* (2008), normal human myoblasts maintain their capability to fuse and differentiate after many passages in culture, when they reach replicative ageing and stop dividing: young myoblasts were found to form very long and branched myotubes, about 90% of the myonuclei being contained in myotubes with more than 50 nuclei; senescent normal myoblasts formed much shorter myotubes, and less than 40% of the myonuclei were found in myotubes with 25 nuclei or more. This suggests the occurrence of a defect in the differentiation and/or fusion capabilities of normal myoblasts as long as they become senescent (Bigot *et al.*, 2008). Our results are consistent with these observations, but also indicates that even the proliferating M9 myoblasts from DM2 patients form much shorter myotubes with a relatively low number of nuclei. In addition, already at a relatively early differentiation step (T12) the myotubes derived from M12 myoblasts showed features suggestive of degenerating myotubes: i.e., cytoskeleton disorganization, small mitochondria with a few recognizable cristae, and
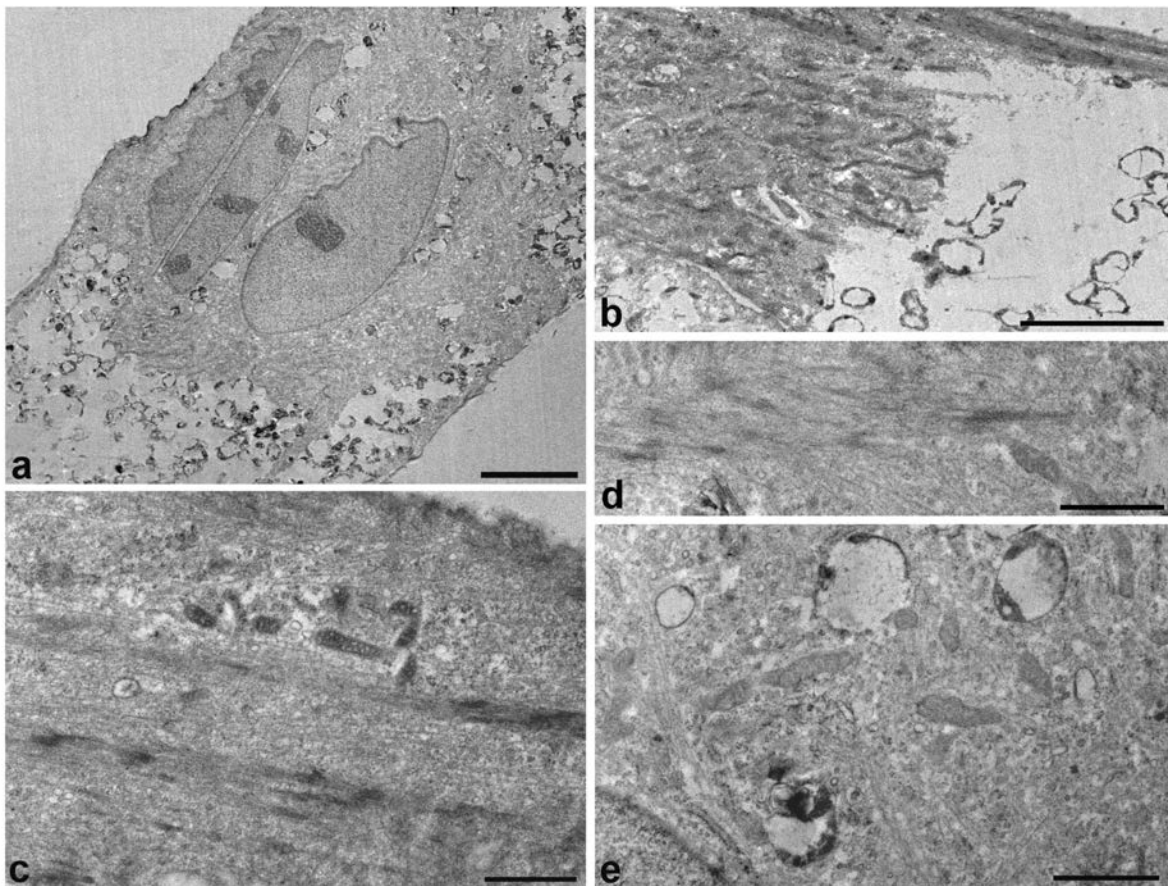
Figure 3. Electron micrographs of myotubes derived by M12 myoblasts at the differentiation step T8 (a-c), T12 (d) and T22 (e). (a) Myotube with 3 transversally aligned nuclei. (b) Cytoplasmic areas containing the usual organelles are close to wide, electron-lucent regions containing heterogeneous vacuoles. (c) Myofibril bundles are thin and show a few sarcomeric-like arrangements; small mitochondria are distributed as clusters. (d) In T12 myotubes the myofibrils are disorganized. (e) In T22 myotubes mitochondria contain hardly recognizable cristae, smooth vesicles are numerous, and free ribosomes and RER are abundant. Bars: (a,b) 5 μm, (c-e) 1 μm.

large amounts of heterogeneous vacuoles. At the subsequent steps in differentiation medium, cytoplasmic degeneration became more apparent; however, it is worth noting that the proteosynthetic apparatus as well as the cell nuclei did not seemed to be severely affected even at the latest differentiation times analyzed; even the mitochondrial population was only partially damaged at T22, and a fraction of mitochondria preserved their normal intermembrane potential, as demonstrated by JC1 staining. Interestingly, no structural alteration typical of apoptotic cell death (Burattini *et al.*, 2004; D'Emilio *et al.*, 2010) was found in our experimental conditions, contrary to what observed in 15-day differentiated DM1 myotubes (Loro *et al.*, 2010). This difference could be related to the more severe consequences of the nuclear sequestration of defective mRNA in the nuclei of DM1 compared to DM2 cells.

In conclusion, our study confirms and extends previous data showing that DM2 myoblasts in culture can be induced to differentiate into myotubes (Cardani *et al.*, 2009; Pelletier *et al.*, 2009), but their differentiation potential markedly decreases in parallel with their senescence *in vitro*. The structural alterations early observed in the myotubes from senesceing myoblasts suggest that also *in vivo* the differentiation potential of satellite cells in DM2 patients could be low, thus compromising their capability to repair dystrophic muscles.

Acknowledgments

References

Bigot A, Jacquemin V, Debacq-Chainiaux F, Butler-Browne GS, Toussaint O, Furling D, Mouly V. Replicative aging down-regulates the myogenic regulatory factors in human myoblasts. Biol Cell 2008;100:189-99.

Bischoff R, Heintz C. Enhancement of skeletal muscle rigeneration. Dev Dyn 1994;201:41-54.

Burattini S, Ferri P, Battistelli M, Curci R, Luchetti F, Falcieri E. C2C12 murine myoblasts as a model of skeletal muscle development: morpho-functional characterization. Eur J Histochem 2004;48:223-33.

Cardani R, Baldassa S, Botta A, Rinaldi F, Novelli G, Mancinelli E, et al. Ribonuclear inclusions and MBNL1 nuclear sequestration do not affect myoblast differentiation but alter gene splicing in myotonic dystrophy type 2. Neuromuscul Disord 2009;19:335-43.

Cardani R, Mancinelli E, Sansone V, Rotondo G, Meola G. Biomolecular identification of (CCTG)n mutation in myotonic dystrophy type 2 (DM2) by FISH on muscle biopsy. Eur J Histochem 2004;48:437-42.

Cardani R, Mancinelli E, Rotondo G, Sansone V, Meola G. Muscleblind-like protein 1 nuclear sequestration is a molecular pathology marker of DM1 and DM2. Eur J Histochem 2006;50:177-82.

Cooper RN, Tajbakhsh S, Mouly V, Cossu G, Buckingham M, Butler-Browne GS.In vivo satellite cell activation via Myf5 and MyoD in rigenerating mouse skeletal muscle. J Cell Sci 1999;112:2895-901.

Curci R, Battistelli M, Burattini S, D'Emilio A, Ferri P, Lattanzi D, et al. Surface and inner cell behaviour along skeletal muscle cell in vitro differentiation. Micron 2008;39:843-51

D'Emilio A, Biagiotti L, Burattini S, Battistelli M, Canonico B, Evangelisti C, et al. Morphological and biochemical patterns in skeletal muscle apoptosis. Histol Histopathol 2010;25:21-32.

Fardaei M, Rogers MT, Thorpe HM, Larkin K, Hamshere MG, Harper PS, et al. Three proteins, MBNL, MBLL and MBXL, co-localize in vivo with nuclear foci of expanded-repeat transcripts in DM1 and DM2 cells. Hum Mol Gen 2002;11:805-14.

Harper PS. Myotonic Dystrophy, 3rd ed, WB Saunders, London, 2001.

Jacob WA, Bakker A, Hertsens RC, Biermans W. Mitochondrial matrix granules: their behaviour during changing metabolic situations and their relationship to contact sites between inner and outer mitochondrial membranes. Microsc Res Tech 1994;27:307-18.

Jameson CW. Towards a unified and interdisciplinary model of ageing. Med Hypotheses 2004;63:83-6.

Liquori CL, Ricker K, Moseley ML, Jacobsen JF, Kress W, Naylor SL, et al. Myotonic dystrophy type 2 caused by a CCTG expansion in intron 1 of ZNF9. Science 2001;293:864-7.

Loro E, Rinaldi F, Malena A, Masiero E, Novelli G, Angelini XC., et al. Normal myogenesis and increate

apoptosis in myotonic dystrophy type-1 muscle cells. Cell Death Diff 2010;doi: 10.1038/cdd.2010.33.

Machida S, Narusawa M. The roles of satellite cells and hematopoietic stem cells in impaired regeneration of skeletal muscle in old rats. Ann New York Acad Sci 2006;1067:349–53.

Malatesta M, Battistelli S, Rocchi MBL, Zancanaro C, Fakan S, Gazzanelli G. Fine structural modifications of liver, pancreas and brown adipose tissue mitochondria from hibernating, arousing and euthermic dormice. Cell Biol Int 2001;25:131-8.

Mankodi A, Teng-Umnuay P, Krym M, Henderson D, Swanson M, Thornton CA. Ribonuclear inclusions in skeletal muscle in myotonic dystrophy types 1 and 2. Ann Neurol 2003;54:760-8.

Mankodi A, Urbinati CR, Yuan QP, Moxley RT, Sansone V, Krym M, et al. Muscleblind localizes to nuclear foci of aberrant RNA in myotonic dystrophy types 1 and 2. Hum Mol Genet 2001;10:2165-70.

Moss FP, Leblond CP. Satellite cells as the source of nuclei in muscles of growing rats. Anat Rec 1971;170:421-35.

Moxley 3rd RT, Meola G, Udd B, Ricker K. Report of the 84th ENMC workshop: PROMM (proximal myotonic myopathy) and other myotonic dystrophy-like syndromes: 2nd workshop. 13–15th October 2000, Loosdrecht: The Netherlands. Neuromuscul Disord 2002;12:306–17.

Pascual M, Vicente M, Monferrer L, Artero R. The Muscleblind family of proteins: an emerging class of regulators of developmentally programmed alternative splicing. Differentiation 2006;74:65-80.

Pelletier R, Hamel F, Beaulieu D, Patry L, Haineault C, Tarnopolsky M, et al. Absence of a differentiation defect in muscle satellite cells from DM2 patients. Neurobiol Dis 2009;36:181-90.

Perdoni F, Cardani R, Giagnacovo M, Veneroni P, Meola G, Pellicciari C, Malatesta M. Ultrastructural characterization of the MBNL1-containing foci occurring in myoblast and myotube nuclei from patients affected by myotonic dystrophy type 2. Microscopie, 2009a;11:60-4.

Perdoni F, Malatesta M, Cardani R, Giagnacovo M, Mancinelli E, Meola G, Pellicciari C. RNA/MBNL1-containing foci in myoblast nuclei from patients affected by myotonic dystrophy type 2: an immunocytochemical study. Eur J Histochem 2009b;53:151-8.

Ranum LP, Cooper TA. RNA-mediated neuromuscular disorders. Annu Rev Neurosci 2006;29:259-77.

Reers M, Smith, TW, Chen LB. J-aggregate formation of a carbocyanine as a quantitative fluorescent indicator of membrane potential. Biochemistry 1991;30:4480-6.

Schultz E, Lipton BH. Skeletal muscle satellite cells: changes in proliferation potential as a function of age. Mech Ageing Dev 1982;20:377-83.

Verdijk LB, Koopman R, Schaart G, Meijer K, Savelberg HH, van Loon LJ. Satellite cell content is specifically reduced in type II skeletal muscle fibers in the elderly. Am J Physiol Endocrinol Metab 2007;292:E151-7.

Wheeler TM, Thornton CA. Myotonic dystrophy: RNA-mediated muscle disease. Curr Opin Neurol 2007;20:572-6.